TWO NEW DESIGNS OF PARABOLIC SOLAR COLLECTORS

by

Omid KARIMI SADAGHIYANI [a]*, Mohammad Bagher SADEGHI AZAD [b], Sharam KHALILARIA [c], and Iraj MIRZAEE [c]

[a] Department of Mechanical Engineering, Khoy Branch, Islamic Azad University, Khoy Iran
[b] Department of Mechanical Engineering, Urmia University of Technology, Urmia, Iran
[c] Department of Mechanical Engineering, Urmia University, Urmia, Iran

Original scientific paper
DOI: 10.2298/TSCI111105089S

In this work, two new compound parabolic trough and dish solar collectors are p resented with their working principles. First, the curves of mirrors are defined and the mathematical formulation as one analytical method is used to trace the sun rays and recognize the focus point. As a result of the ray tracing, the distribution of heat flux around the inner wall can be reached. Next, the heat fluxes are calculated versus several absorption coefficients. These heat flux distributions around absorber tube are functions of angle in polar co-ordinate system. Considering, the achieved heat flux distribution are used as a thermal boundary condition. After that, finite volume methods is applied for simulation of absorber tube. The validation of solving method is done by comparing with Dudley's results at Sandia National Research Laboratory. Also, in order to have a good comparison between LS-2 and two new designed collectors, some of their parameters are considered equal with together. These parameters are consist of: the aperture area, the measures of tube geometry, the thermal properties of absorber tube, the working fluid, the solar radiation intensity and the mass flow rate of LS-2 collector are applied for simulation of the new presented collectors. After the validation of the used numerical models, this method is applied to simulation of the new designed models. Finally, the outlet results of new designed collector are compared with LS-2 classic collector. Obviously, the obtained results from the comparison show the improving of the new designed parabolic collectors efficiency. In the best case-study, the improving of efficiency are about 10% and 20% for linear and convoluted models, respectively.

Key words: *compound parabolic concentrator, collector efficiency, blackbody theory, ray tracing, CFD modeling*

Introduction

In order to heighten the properties of a parabolic trough collector, it is necessary to conquer its restrictions and reduce the high accuracy requirement of the solar tracking system. A new kind of compound parabolic concentrator (CPC) is presented in this work.

In the field of concentrating solar collectors, Richter [1] introduced and investigated the ordinaryparabolic trough solar concentrator as one of the most advanced technologies in 1996. These solar concentrators has been analyzed in many large scale solar power-plants by Price *et al*. [2] and Schwartzer *et al*. [3].

The configuration of solar energy collectors is constructed by one mathematical curve, for example, a parabolic dish and trough concentrators [4]. These kinds of solar systems are simple and efficient but full of restrictions. These limitations include problems with dust collec-

*Corresponding author; e-mail: st_o.sadaghiyani@urmia.ac.ir

tion, wind resistance and control difficulties. In 1974, Winston [5] invented the CPC that traced the sun with rotation and movement. Some from of tracking systems is used to enable the collector to follow the sun. If the solar incident rays cannot be reflected correctly to the tube receiver, the reflection will be useless. In order to advantage the ordinary parabolic trough concentrator and conquer its disadvantage and also decrease the error tracing, the track precision is required [6]. In this work, two new imaging compound parabolic trough concentrators are designed. The most important prospect of the collectors is that the single curved concentrating surface in the usual parabolic trough and dish collectors replaced with a multiple curved that focus sun rays. These methods help basically to reach to a more homogenous heat flux distribution around the receiver tube. To decrease heat dissipation an evacuation tube is used and, based on the results of Jeter [7], it is assumed that the sun rays are parallel.

The new solar collector designs

Definition of LS-2 parabolic trough concentrator

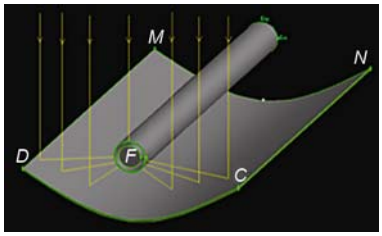

Figure 1. LS-2 parabolic trough concentrator tested at SNRL

Figure 1 shows the schematically a traditional parabolic trough concentrator, which is made by bending a sheet of reflective material with reflectivity 96%.

The LS-2 parabolic trough concentrator (PTC) tested at Sandia National Laboratory by Dudley *et al*. [8] was selected as a basic simulation. Its geometric characteristics and operation parameters are listed in tab. 1.

The performance of the tracking mechanism is assumed to work very well. Optical errors could be eliminated and the incident angle modifier could be assumed to be one.

Table 1. Characteristics of the LS-2 parabolic solar collector

LS-2 PTC			
Manufacturer	Luz industrial-Israel	Absorber diameter	70 mm
Operating temperature	100-400 °C	Diameter of glass cover	115 mm
Module size	7.8 m × 5 m	Transmittance of glass cover	0.95
Rim angle	70 degrees	Absorber surface	Cermet selective surface
Reflector	12 thermally sagged glass panel with reflectivity 0.96	Absorptivity of absorber tube	0.96
Aperture area	39.2 m^2	Absorber tube inner diameter	66 mm
Focal length	1.84 m	Absorber tube outer diameter	70 mm
Concentration ratio	22.74	Flow restriction device (plug)diameter	50.8 mm
Receiver	Evacuated tube, metal bellows at each end		

Presentation of the new parabolic collector designs

In this work, two new models are presented that their functions are based on blackbody theory. In these models, the sun rays are concentrated on linear path after reflecting from two faces. The two new designs of parabolic compound solar collector are: (a) linear model and (b) convoluted model of compound parabolic collector, presented in fig. 2.

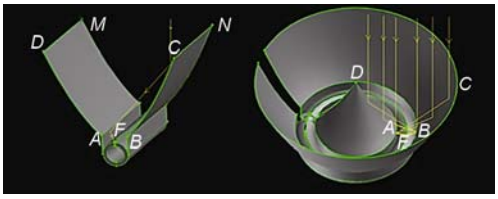

(a) (b)

Figure 2. Two new parabolic concentrators (a) Linear model and (b) Convoluted model (for color image see journal web-site)

One linear slit traps reflected rays. The rays after several reflecting are absorbed at the inner wall of the absorber tube. Therefore, the distribution of radiation heat flux is calculated by simulating the radiation around the absorber tube inner wall. Consider that, the ray tracing process via mathematical method is presented in Appendix.

Absorber tube

In order to reach to good comparison, the geometrical amounts of absorber tube in LS-2 collector are used in presented models. Figure 3 shows the absorber tube of two new designed collectors and compare of them with absorber tube of LS-2.

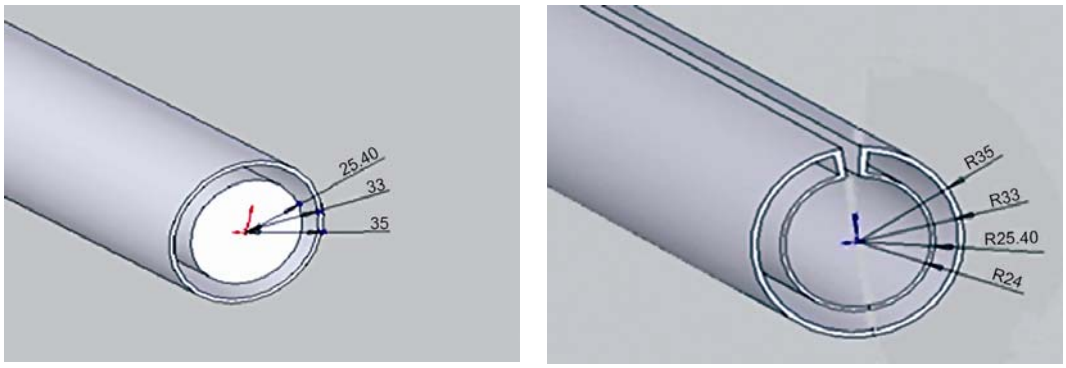

(a) (b)

Figure 3. Schematics of the absorber tube of (a) the LS-2 collector and (b) the new design

But in this work, the absorber tubes with suitable absorptivity and high reflectivity is used. So primarily, LS-2 collector geometry is modeled and simulated with computational fluid dynamics (CFD) as finite volume numerical method with structured grids.

After validation of solving method, the amounts of direct normal irradiance (DNI), the aperture area and inlet temperature that are used in LS-2 collector models, will be applied in two new designed models.

CFD modeling

Governing equations

Assuming steady-state turbulent flow, the governing equations for continuity, momentum, energy and standard k-ε turbulence model can be written as [9]:

– continuity equation

$$\frac{\partial}{\partial x_i}(\rho u_i) = 0 \tag{1}$$

– momentum equation

$$\frac{\partial}{\partial x_i}(\rho u_i u_j) = -\frac{\partial p}{\partial x_i} + \frac{\partial}{\partial x_i}\left[(\mu_t + \mu)\left(\frac{\partial u_i}{\partial x_j} + \frac{\partial u_j}{\partial x_i}\right) - \frac{2}{3}(\mu_t + \mu)\frac{\partial u_l}{\partial x_l}\delta_{ij}\right] + \rho g_i \tag{2}$$

– energy equation

$$\frac{\partial}{\partial x_i}(\rho u_i T) = \frac{\partial}{\partial x_i}\left[\left(\frac{\mu}{\mathrm{Pr}} + \frac{\mu_t}{\sigma_T}\right)\frac{\partial T}{\partial x_i}\right] + S_R \tag{3}$$

– k equation

$$\frac{\partial}{\partial x_i}(\rho u_i k) = \frac{\partial}{\partial x_i}\left[\left(\mu + \frac{\mu_t}{\sigma_k}\right)\frac{\partial k}{\partial x_i}\right] + G_k - \rho\varepsilon \tag{4}$$

– εequation

$$\frac{\partial}{\partial x_i}(\rho u_i \varepsilon) = \frac{\partial}{\partial x_i}\left[\left(\mu + \frac{\mu_t}{\sigma_\varepsilon}\right)\frac{\partial \varepsilon}{\partial x_i}\right] + \frac{\varepsilon}{k}(c_1 G_k - c_2 \rho\varepsilon) \tag{5}$$

where the turbulence viscosity and the production rate are expressed by:

$$\mu_t = c_\mu \rho \frac{k^2}{\varepsilon} \tag{6}$$

$$G_k = \mu_t \frac{\partial u_i}{\partial x_j}\left(\frac{\partial u_i}{\partial x_j} + \frac{\partial u_j}{\partial x_i}\right) \tag{7}$$

The standard turbulence model constants are used: c_μ = 0.09,c_1 = 1.44, c_2 = 1.92, σ_k = 1.0, σ_ε = 1.3, andσ_T = 0.85.

Simulation of LS-2 collector

In order to validate the in-house computational code, LS-2 SEGS collector is selected. The computational domain contains the absorber tube (solid), the working fluid domain (fluid) and flow restriction device (solid). For grid independence test, four different grid systems were created and investigated as:

(N_c = 70, N_z = 340), (N_c = 70, N_z = 430), (N_c = 70, N_z = 500), and (N_c = 90, N_z = 340)

Results show good agreement with together and grid independency has been demonstrated. The fundamental equations were discretized by the finite volume method [10] and the convective terms in momentum and energy equations were discretized *via* the second upwind scheme. The algorithm of SIMPLE was used to coupling between pressure and velocity. Con-

sider that, the convergence scale for the velocity and energy was the maximum residual of the first 10 iterations was less than $10^{-5}$and 10^{-7}, respectively. Hence, after simulation its outlet results are compared with Dudley's experimental results. The comparison between outlet temperature and efficiency of numerical simulation and experimental results shows the reasonable agreement together. Because of this good agreement, the numerical solving method is validated. Table 2 shows the demonstration of validation.

Table 2. Comparison of present numerical results with Dudley's [8]

DNI [Wm^{-2}]	Mass flow rate [kgs^{-1}]	Inlet temperature [K]	Outlet temperature experimental [K]	Outlet temperature-numerical [K]	η [%] Efficiency experimental	η [%] Efficiency theoretical
933.7	0.6782	375.5	397.5	399	72.07	74
982.3	0.7205	471	493	495.7	71	73.4
909.5	0.81	524.2	542.9	546.1	70.5	72.1

This numerical solving method is applied for simulation of two new designed models.

Boundary conditions of the new designs

The boundary conditions that are applied to the inlet and outlet cross-section of collector tube:

– for inlet

$$\dot{m}_{in} = \dot{m}_z = 0.6782 \text{ kg/s (mass flow inlet)}, \quad \dot{m}_x = \dot{m}_y = 0 \text{ kg/s}, \quad T_{in} = 375.5 \text{ K} \tag{8}$$

Turbulent kinetic energy: $k_{in} = 1\%$ of the $(1/2)u_{in}^2$.

Turbulent dissipation rate: $\varepsilon_{in} = c_\mu \rho(T) k_{in}^2 / \mu_t$.

Considering:

$$c_\mu = 0.09, \quad \mu_t = 100 \tag{9}$$

– foroutlet –fully-developed assumption (outflow).

– forwalls –two ends of the receiver tube; adiabatic walls.

– forinner wall of receiver tube –heat flux wall which is calculated by MATLAB in-house code and outer wall is isolated.

The amount of direct normal intensity (DNI) that is used to simulate sun rays is 933 [Wm^{-2}]. The heat transfer fluid (HTF) is Syltherm-800 liquid oil that its physical and thermal properties are functions of temperature as:

$$c_p = 0.00178T + 1.107798 \text{ [kJkg}^{-1}\text{K}^{-1}\text{]} \tag{10}$$

$$\rho = -0.4153495T + 1105.702 \text{ [kg·m}^{-3}\text{]} \tag{11}$$

$$K = -5.753496 \cdot 10^{-10} T^2 - 1.875266 \cdot 10^{-4} T + 0.1900210 \text{ [Wm}^{-1}\text{K}^{-1}\text{]} \tag{12}$$

$$\mu = 6.672 \cdot 10^{-13} T^4 - 1.5661.388 \cdot 10^{-6} T^2 - 5.541 \cdot 10^{-4} T - 8.487 \cdot 10^{-2} \text{[Nsm}^{-1}\text{]} \tag{13}$$

The material of absorber tube is stainless steel-304 with conductivity 54 W/mK. Also, in order to reach to the best absorption coefficient, the several coatings are considered

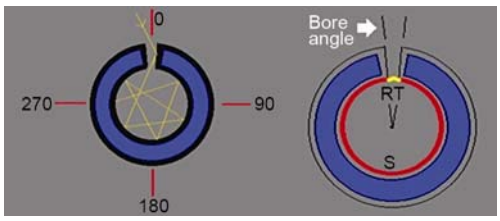

(a) (b)

Figure 4. Schematics of (a) one ray path in the absorber tube and (b) the bore angle
(for color image see journal web-site)

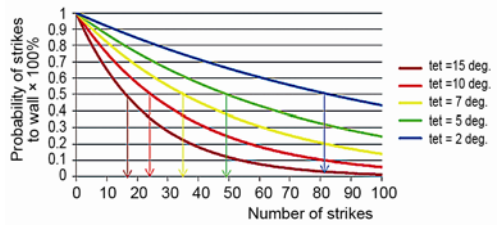

Figure 5. The probability of ray strikes to wall
(for color image see journal web-site)

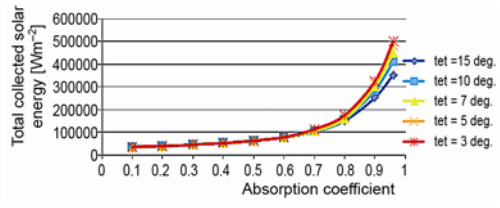

Figure 6. Total solar energy *vs.* absorptivity and bore angle
(for color image see journal web-site)

for inner surface. Figure 4 shows the path of one arbitrary sun ray and measurement of angles schematically.

The probability function for n-time strikes is exponential function:

Probability of n-time strikesq^{n-1} (14)

where q is the probability of strike to the tube wall which can be reached based on probability on continuous space:

$$\frac{\text{RST}\ \ [\text{red arc in fig. 4(b)}]}{2\pi r_i} \tag{15}$$

After calculation of q for each of bore angles, the exponential probability function can be reached. Thus, the achieved functions are plotted and presented at fig. 5. In order to simplification of analyses, probability= 0.5 and its number of strikes are considered. Based on this assumption, the number of strikes are reached and applied for calculation of total solar radiation energy. The solar radiation energy is converted into wall heat flux. The diagrams of heat flux are the results of this simulation which are presented below for linear and convoluted model separately.

The numbers of strikes *vs.* probability = 0.5 are shown in fig. 5. These numbers are 16, 24, 35, 49, and 83. Therefore, total solar radiation energies are calculated *vs.* several bore angles. Figure 6 shows the total solar energies. The total solar energy is the summation of geometrical progression terms as follow:

– Geometric concentration

$$\frac{\text{the wide of collector}}{\text{the circumference of absorber surface}} = \frac{5000\ \text{mm}}{2\ \pi \times 24\ \text{mm}} = 33.158 \tag{16}$$

– Total heat flux that arrive from bore at one second is:

$$DNI \times GC = 933.7 \times 33.158 = 30959.62 \tag{17}$$

The summation of geometrical progression terms:

$$\frac{DNI\ (1 - r^n)}{1 - r} \tag{18}$$

In mathematical r is named progression coefficient and in optical models can be equal with the absorption coefficient of surface. The results of these formulations are given in fig. 6.

The first step for simulation of LS-2 and two new presented models is specification of heat flux distribution. Therefore, in order to achievement to heat flux function, in polar coordination system the MATLAB code must be written to specify distribution of solar heat flux. In order to study the effect of tube surface material, several absorption coefficients are considered and calculated. After the run of MATLAB code the results are given for linear and convoluted absorber tubes in figs. 7 and 8.

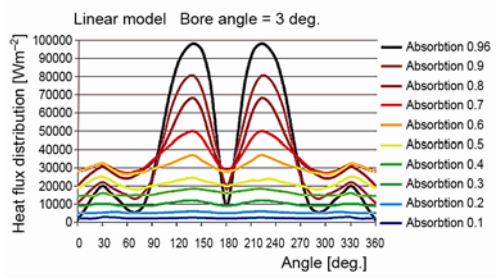

Figure 7. Distribution of heat flux around inner wall of linear absorber tube versus angleand absorption coefficients
(for color image see journal web-site)

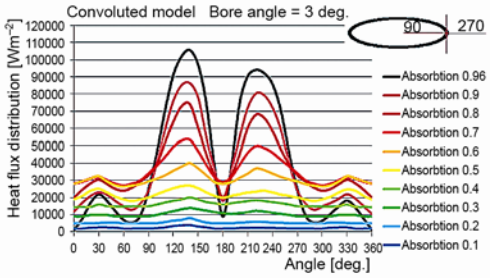

Figure 8. Distribution of heat flux around inner wall of convoluted absorber tube *versus* angle and absorption coefficients
(for color image see journal web-site)

Numerical simulation of two new presented models

The new models must be simulated and compared with LS-2 PTC. The mass flow rate, direct normal intensity (DNI), the amounts of tube diameters, the reflectivity of mirror and the area of mirror are considered equal with LS-2 PTC. The used and validated numerical method for LS-2 collector is applied for simulation of two presented models. Therefore, the outlet temperature and efficiency of collectors are comparison criterion. The definition of collector efficiency is:

– the efficiency of collectors (%)

$$\frac{\dot{m}C_p(T_o - T_i)}{DNI \times A_c} \times 100\% \tag{19}$$

After the simulation and calculation of collector efficiency, the results are presented at figs. 7 and 8, respectively.

After that, the all case studies are simulated *via* the finite volume methods as a CFD technique. The aim of numerical simulations is the investigation of absorption coefficient (α) and collector shape effects on the outlet temperature and efficiency (figs. 9 and 10). Therefore, the geometry of absorber tube is generated and the finite volume methods (FVM) are established to simulate all case studies.

The achieved results show that, the absorption coefficients =0.8 gives the maximum outlet temperature and efficiency in the both models (linear and convoluted). The trend of diagram decreases *vs.* absorption coefficients>0.8. Its reason is the quality of heat flux distribution. It is concluded, the homogeny of heat flux distribution effects on outlet temperature

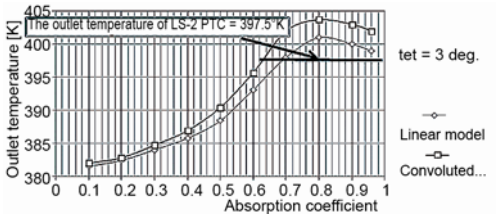

Figure 9. Comparison of outlet temperature of the new designs with that LS-2 PTC

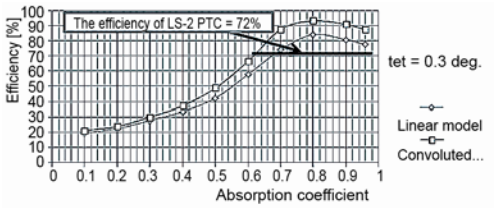

Figure 10. Comparison of efficiency of the new designs with that LS-2 PTC

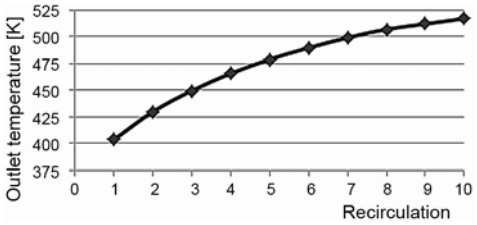

Figure 11. Effect of number of recirculation on outlet temperature of convoluted collector

and efficiency of collectors. With the decrease in absorption coefficients, the heat flux distribution will approximately be homogenous. In other words, in the homogenous heat flux distribution the working fluid is heated better than non-homogenous. Therefore, the homogeny of heat flux distribution *vs.* absorptivity = 0.8 is more than absorptivity = 0.9 and 1. Also, the decreasing of absorption coefficients leads to decreasing of the amount of absorbed solar energy.

Consider that, because of circulated path, the convoluted model gives high outlet temperature rather than the linear model. Also, the other prominence of convoluted model *vs.*linear model is that the high outlet temperatures can be reached via the several recirculation of fluid flow. This influence of recirculation number is shown in fig. 11.

Conclusions

In this work, based on black body theory, two new models are designed and presented. The aim of these models presentation, is improving the outlet temperature and efficiency of compound parabolic concentrators which are compared with LS-2 results.

For linear model and for absorption confidents >0.8 and bore angles <3°, the outlet temperature and efficiency are higher than LS-2 collector. Because, the homogeneous heat flux and high absorption coefficients of absorber surface leads to increasing and improving of outlet parameters.

For convolute collector the outlet temperature and efficiency are higher than LS-2 collector and linear model due to convoluted path and uniform heat flux.

In convoluted collector because of several circulation of flow the outlet temperature increases continuously.

Nomenclature

A_c – aperture area
c_μ, c_1, c_2 – coefficients in the turbulence model
DNI – direct normal intensity, [Wm^{-2}]
g – gravity, [ms^{-2}]
k – thermal conductivity or kinetic energy
$\dot{m}$ – mass flow rate, [kgs^{-1}]
S_R – additional source term, [Wm^{-3}]
T – temperature, [K]
tet – bore angle
u, v, w – velocity components, [ms^{-1}]
x, y, z – Cartesian co-ordinates

Greek symbols

ε – turbulent dissipation rate or emissivity
μ – dynamic viscosity, [Pas]

μ_t – turbulent viscosity, [Pas]
ρ – density, [kgm^{-3}]
ν – kinematic viscosity, [m^{2}s^{-1}]
σ_T – turbulent Prandtl number
σ_k, σ_ε – turbulent Prandtl numbers for diffusion of k and □
η – collector efficiency calculated by test data

Subscripts

in – inlet parameters
m – mean or average value
o – outlet parameters
c – circumference
ex – experimental
nu – numerical
z – longitudinal

Appendix

Mathematical analysis of the new collector geometries

Model geometry and ray tracing

The parallel sun rays at a direction of symmetric axis (y) incident to the parabolic mirrors. Then, the reflected rays osculate to the vertical mirrors as (AN) and (BM). Finally, they are focused at liner path located at F point. Figure 12 shows the sun rays and their paths after reflection. This mirror contains two parabolic curves that are symmetrically displaced.

Figure 12 exhibits the cross section of the new concentrator. The x-y co-ordinate system is established. Curves (DA) and (CB) are the sections of two parabolic curves with equal size and upturned aperture. F_1 and $F_2$are two focus points of parabolic shapes. The formulation of these parabolic curves can be expressed by:

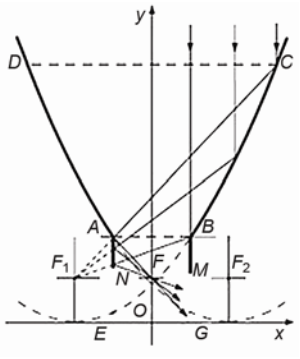

Figure 12. Schematic of the new presented compound parabolic concentrator

$$\text{for } (AD): y = \frac{1}{4f}(x+a)^2 \tag{20}$$

$$\text{for } (BC): y = \frac{1}{4f}(x-a)^2 \tag{21}$$

where f is the focal length of parabolic curves, and a is the displacement of the curves on the x axis. In this case, the movement of each curves must be equal with $|F_1F_2|/2 = a$.

The rays after reflection stoke the linear selection. These linear sections are parallel with the y axis. In order to make the sunlight directly radiating trough AB section, the amount of AB aperture width must be a and the slit of receiver must be located on Fpoint. In fig. 14, y_B can be reached by:

$$y_B = \frac{1}{4f}(x_B + a)^2 = \frac{1}{4f}\left(\frac{a}{2} + a\right)^2 = \frac{9a^2}{16f} \tag{22}$$

The y- co-ordinate of point B must be greater than focal length, so:

$$\frac{9a^2}{16f} > f \tag{23}$$

In other words:

$$0 < \frac{f}{a} < \frac{3}{4} \tag{24}$$

Consider that, the rays are reflected by parabolic surface (CB) to flat surface (AN). Therefore, the minimum height of the secondary reflection surface (AN) must be the length of (AN). The position of point N can be determined by the point of crossover of line BF_1 and AE. The equation of $BF_1$is:

$$\frac{y - y_{F_1}}{x - x_{F_1}} = \frac{y_{F_1} - y_B}{x_{F_1} - x_B} \tag{25}$$

$$\frac{y - f}{x - a} = \frac{f - \dfrac{9a^2}{16f}}{a + \dfrac{a}{2}} \tag{26}$$

So after simplification:

$$y = \left(\frac{3a}{8f} - \frac{2f}{3a}\right)x + \frac{3a^2}{8f} + \frac{f}{3} \tag{27}$$

Also, the equation of AE line is:$x = -a/2$.
So the co-ordination of intersection point of AE and BF_1 is calculated:

$$y_N = \frac{3a^2}{16f} + \frac{2f}{3} \tag{28}$$

Then, the height of secondary vertical surface must be:

$$h = y_A - y_N > \frac{9a^2}{16f} - \frac{3a^2}{16f} - \frac{2f}{3} = \frac{3a^2}{8f} - \frac{2f}{3} \tag{29}$$

The co-ordination of A point:

$$x_A = -\frac{a}{2} \tag{30}$$

$$y_A = \frac{1}{4f}(x_A - a)^2 = \frac{1}{4f}\left(\frac{a}{2} - a\right)^2 = \frac{9a^2}{16f} \tag{31}$$

The co-ordination of F_1 point:

$$x_{F_1} = -a \tag{32}$$

$$y_{F_1} = f \tag{33}$$

Linear model

The dimension of aperture area (CD) is as large as LS-2 collector and (5 m) and the length of this trough collector (CN) is 7.8m. Based on eqs. (20) to (33), one compound parabolic concentrator with certain dimensions is presented. If f = 0.52 m, and a = 0.7 m, then:

$$y = \frac{1}{2.08}(x + 0.7)^2 \tag{34}$$

$$y = \frac{1}{2.08}(x - 0.7)^2 \tag{35}$$

Because of x_C = 2.5m, and x_D = –2.5m, and using eqs. (20) and (21), the amounts ofy_C and y_D become 4.92m. The focal length (f) and curves displacement (a) satisfy the limitation relation (5):

$$0 < \frac{f}{a} < \frac{3}{4} \rightarrow 0 < \frac{0.52}{0.7} < \frac{3}{4} \rightarrow 0 < 0.7428 < 0.75$$

and

$$x_A = -0.35 \text{ m}, \quad y_A = 0.523 \text{ m}, \quad x_N = -0.35 \text{ m}, \quad y_N = 53 \text{ m}, \quad \text{therefore } h > 0.007 \text{ m} \tag{36}$$

Also, the co-ordination of focus points F_1 and F_2 are:

$$x_{F_1} = -0.7 \text{ m}, \quad y_{F_1} = 0.52 \text{ m}, \quad \text{and} \quad x_{F_2} = 0.7 \text{ m}, \quad y_{F_2} = 0.52 \text{ m} \tag{37}$$

Consider that, h has very little amount and the focusing of sun rays has been done successfully.

Convoluted model

In this case, it is assumed that, the area of circular aperture becomes 39.2 m^2as large as LS-2 collector. Thus, the radius of dish (CD) is 3.53m. According to fundamental equations of parabolic surfaces, by considering f = 0.52 m, and a = 0.7 m, which conclusions are reached as:

$$y = \frac{1}{2.08}(x + 0.7)^2 \tag{38}$$

$$y = \frac{1}{2.08}(x - 0.7)^2 \tag{39}$$

If $|CD|$ = 3.53 m, the co-ordination of points C and D will be:

$$x_C = 1.765 \text{ m and } y_C = 2.92 \text{ m} \tag{40}$$

The coordination of point D:

$$x_D = -1.765 \text{ m and } y_D = 2.92 \text{ m} \tag{41}$$

Also, the co-ordination of focus points are:

$$x_{F_1} = 0.7 \text{ m and } y_{F_1} = 0.52 \text{ m} \tag{42}$$

$$x_{F_2} = 0.7 \text{ m and } y_{F_2} = 0.52 \text{ m} \tag{43}$$

and

$$x_A = -0.35 \text{ m}, \; y_A = 0.53 \text{ m}, \; x_N = -0.35 \text{ m}, \; y_N = 0.523 \text{ m}, \; \text{therefore } h > 0.007 \text{ m} \tag{44}$$

References

[1] Richter, J. L., Optics of a Two-trough Solar Concentrator, *Solar Energy, 56* (1996), 2, pp. 191-198
[2] Price, H., *et al*., Advances in Parabolic Trough Solar Power Technology, *Journal of Solar Energy Engineering, 124* (2002), 5, pp. 109-125
[3] Schwarzer, K., *et al.*, Characterization and Design Methods of Solar Cookers, *Solar Energy, 82* (2008), 2, pp. 157-163
[4] Kaiyan, H., *et al*., An Imaging Compounding Parabolic Concentrator, *Proceedings,*ISES Solar World Congress, Beijing, Vol. 2, 2007, pp. 589-592
[5] Winston, R., Principles of Solar Concentrators of a Novel Design*, Solar Energy, 16* (1974), 2, pp. 89-95
[6] Fraidenraich, N., *et al*., Analytic Solutions for the Geometric and Optical Properties of Stationary Compound Parabolic Concentrators with Fully Illuminated Inverted V Receiver, *Solar Energy, 82* (2008), 2, pp. 132-143
[7] Jetter, S.M., Calculation of the Concentrated Flux Distribution in Parabolic trough Collectors by a Semi-finite Formulation, *Solar Energy*, 37 (1986), 5, pp. 335-345
[8] Dudley, V., *et al*., SEGS LS2 Solar Collector-Test Results, Report of Sandia National Laboratories, SANDIA94-1884, USA, 1994
[9] Cheng, Z.D., *et al*, Three-Dimensional Numerical Study of Heat Transfer Characteristics in the Receiver Tube of Parabolic trough Solar Collector,*International Communications in Heat and Mass Transfer*, 37 (2010), 7, pp. 782-787
[10] Tao. W.Q., *Numerical Heat Transfer,*2nded., Xi'an Jiaotong University Press, Xi'an, China, 2001

Paper submitted: November 5, 2011
Paper revised: June 19, 2013
Paper accepted: June 26, 2013